a Varian E109 ESR spectrometer. Samples were prepared either by in situ reduction of the corresponding chloride with triphenylantimony or by dissolving the radical dimer. Spectral simulations, from which hyperfine coupling constant data were extracted, were performed with a program written by Dr. U. M. Oehler, University of Guelph.[8]

X-ray Measurements. Table IV provides a summary of the pertinent crystallographic data. Crystals suitable for X-ray work were grown from $CHCl_3/CH_3CN$. However, the red blocks so obtained lost solvent rapidly; the data crystal was therefore mounted in the presence of a $CH_3CN/CHCl_3$ mixture inside a quartz capillary. For the cell determination, 25 reflections with 2θ in the range 15-35° were measured. The Laue symmetry was shown to be $\bar{3}$ by an initial fast data collection over the entire reciprocal lattice with $2 < \theta < 6°$. The systematic absences (hkl only present if $-h + k + l = 3n$) together with the Laue symmetry allow the space group to be $R\bar{3}$ or $R3$. E statistics indicated $R\bar{3}$, and this was confirmed by the analysis. The data were corrected for Lorentz, polarization, and absorption effects.[15] The structure was solved by direct methods and refined by full-matrix least-squares calculations. With $Z = 9$, the dimer is required to have crystallographic inversion symmetry. Hydrogen atoms were clearly visible in difference maps computed at intermediate stages of the analysis; they were allowed for as riding atoms [with C-H = 0.95 Å and $U_{iso} = 1.1U(C)$]. Only the phosphorus and selenium atoms were refined anisotropically. The presence of two CH_3CN molecules of solvation was noted; one solvent molecule was reasonably well located, but the other was disordered over at least two sites. These solvent atoms were allowed for by including them at the locations obtained from difference maps and allowing their U and occupancy factors to refine. Scattering factors including anomalous scattering were from standard sources.[16]

Acknowledgment. We thank the Natural Sciences and Engineering Research Council of Canada for financial support. We also thank Professors A. W. Cordes and J. F. Richardson for useful discussions.

Supplementary Material Available: Tables SI and SII, listing anisotropic thermal parameters and calculated hydrogen atom positions for 4 (E = Se) (2 pages); a listing of calculated and observed structure factors (12 pages). Ordering information is given on any current masthead page.

(15) Walker, N.; Stuart, D. *Acta Crystallogr.* **1983**, *A39*, 159.

(16) *International Tables for X-ray Crystallography*; Kynoch Press: Birmingham, England, 1974; Vol. 4.

Contribution from the Department of Industrial Chemistry, Faculty of Engineering, Seikei University, Kichijouji-kitamachi, Musashino, Tokyo 180, Japan

Synthesis and Characterization of Chiral 18-Membered-Macrocycle–Lanthanide Complexes: Circular Dichroism and Circularly Polarized Luminescence

Taro Tsubomura, Koichi Yasaku, Takayuki Sato, and Makoto Morita*

Received May 15, 1991

New chiral 18-membered lanthanide–macrocycle complexes were prepared from lanthanide nitrates, 2,6-pyridinedicarboxaldehyde, and chiral 1,2-diaminocyclohexane by template reaction, where the lanthanides are lanthanum(III), europium(III), and terbium(III) ions. The structures of these complexes were characterized by NMR and luminescence spectroscopy to have D_2 molecular symmetry. Strong circularly polarized luminescence was also detected for the Eu(III) and Tb(III) complexes due to the twisted conformation. The absolute chiral structures were determined from CD data. The intramolecular energy-transfer processes were found to occur between π^* electronic states of the ligand and 4f levels of the central lanthanide ions in the Eu(III) and Tb(III) complexes. In addition, a photodecomposition reaction was studied under strong UV laser radiation.

Introduction

Luminescence and circularly polarized luminescence (CPL) spectra are powerful tools to investigate the structures and electronic states of lanthanide complexes in solution.[1,2] However, chiral lanthanide complexes were often found to be in equilibrium with some solvated species or geometrical isomers coexisting in solution. In such a system, it is in principle difficult to study exact chiroptical properties of the complexes even by the sensitive spectroscopic techniques.

In recent years, new lanthanide complexes having 18-membered macrocyclic ligands have been reported by several groups.[3] These complexes are relatively easily prepared by using a template reaction of 2,6-dicarbonylpyridine derivatives and diamines in the presence of lanthanide ions. It is quite reasonable to consider that the macrocyclic complex does have more symmetric and rigid structure than the other complexes containing flexible linear ligands. When chiral diamines were used, a series of chiral ligands could be prepared by template syntheses. Therefore, the chiral macrocyclic complexes are very good materials suited for studying the chiroptical properties of lanthanide complexes in solution. We report the synthesis and spectroscopic study of the chiral macrocyclic lanthanide complexes Ln(*RR*-pydach)$^{3+}$ and Ln(*SS*-pydach)$^{3+}$ including two *trans*-1,2-diaminocyclohexane moieties (*RR*-pydach = 4(*R*),9(*R*),19(*R*),24(*R*)-3,10,18,25,31,32-hexaazapentacyclo[25.3.1.1^{12,24}.0^{4,9}.0^{19,24}]-dotriaconta-1-(31),2,10,12,14,16(32),17,25,27,29-decaene and *SS*-pydach is an enantiomer having 4(*S*),9(*S*),19(*S*),24(*S*) configurations; Ln = Eu, Tb, and La). The structures of the macrocycle complexes are shown in Figure 1. In the course of our study, photophysical properties of the achiral Eu^{3+} macrocycle complex Eu(pyMeen)$^{3+}$ were reported by Sabbatini et al.,[4] where pyMeen = 2,7,13,18-tetramethyl-3,6,14,17,23,24-hexaazatricyclo[17.3.1.1^{8,12}]tetracosa-1(23),2,6,8,10,12(24),13,17,19,21-decaene. In this paper, spectroscopic properties of Eu(pyMeen)$^{3+}$, are also compared with our complexes.

Experimental Section

Lanthanide nitrate hexahydrates were prepared as follows. Lanthanide oxides were dissolved in an excess of nitric acid. The solution was evaporated on a steam bath to give a syrup. After cooling, white crystals obtained were dried in a desiccator and used without further purification. Optical resoltuion of *trans*-1,2-diaminocyclohexane was performed by using L- and D-tartaric acid.[5] Pyridine-2,6-dicarboxaldehyde was synthesized from 2,6-pyridinedimethanol[6] or purchased

(1) (a) Carnall, W. T. In *Handbook on the Physics and Chemistry of Rare Earths*; Gschneider, K. A., Eyring, L., Eds.; North-Holland: Amsterdam, 1979; Vol. 3, p 171. (b) Blasse, G. *Ibid.* North-Holland: Amsterdam, 1979; Vol. 4, p 237. (c) Riel, J. P.; Richardson, F. S. *Chem. Rev.* **1986**, *86*, 1.

(2) (a) Murata, K.; Morita, M.; Eguchi, K. *J. Lumin.* **1984**, *42*, 227. (b) Morita, M.; Eguchi, K.; Shishikura, M.; Nishimura, H.; Inoue, M. *Ibid.* **1984**, *31-32*, 558.

(3) (a) Radecka-Paryzek, W. *Inorg. Chim. Acta* **1980**, *45*, L147. (b) Bombieri, G.; Benetollo, F.; Polo, A.; Cola, L. D.; Vallarino, L. M. *Inorg. Chem.* **1986**, *25*, 1127. (c) Arif, A. M.; Backer-Dirks, J. D. J.; Grey, C. J.; Hart, F. A.; Hursthouse, B. *J. Chem. Soc., Dalton Trans.* **1987**, 1665.

(4) Sabbatini, N.; Cola, L. D.; Vallarino, L. M.; Blasse, G. *J. Phys. Chem.* **1987**, *91*, 4681.

(5) Asparger, R. G.; Liu, C. F. *Inorg. Chem.* **1965**, *4*, 1492.

(6) Papadoupoulous, E. P.; Jarrar, A.; Issidorides, C. H. *J. Org. Chem.* **1966**, *31*, 615.

0020-1669/92/1331-0447$03.00/0

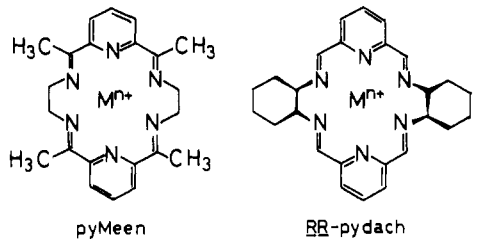

Figure 1. Structures of macrocycle complexes, M = La^{3+}, Eu^{3+}, and Tb^{3+}.

from Aldrich Co. Methanol was dried over 3A molecular sieves.

[Tb(*RR*-pydach)]$(NO_3)_3 \cdot {}^3/_2H_2O$. Terbium(III) nitrate hexahydrate (0.46 g, 1 mmol), 1(*R*),2(*R*)-diaminocyclohexane (0.23 g, 2 mmol), and pyridine-2,6-dicarboxaldehyde (0.27 g, 2 mmol) were dissolved in dry methanol, and the mixture was refluxed for 4 h. The pale yellow solution was cooled to room temperature, and colorless microcrystals obtained by filtration were washed with methanol and ether and dried in vacuo, yield 47%. Anal. Calcd: C, 39.11; H, 4.17; N, 15.78. Found: C, 38.98; H, 3.80; N, 16.13.

[Eu(*RR*-pydach)]$(NO_3)_3$. The complex was prepared by the same procedure as that for [Tb(*RR*-pydach)]$(NO_3)_3 \cdot {}^3/_2H_2O$, yield 34%. Recrystallization from methanol yielded colorless prismic crystals. Anal. Calcd: C, 40.84; H, 3.95; N, 16.48. Found: C, 40.99; H, 3.87; N, 16.54.

[La(*RR*-pydach)]$(NO_3)_3 \cdot 2H_2O$. The complex was prepared by the same procedure as that for [Tb(*RR*-pydach)]$(NO_3)_3 \cdot {}^3/_2H_2O$, yield 33%. Anal. Calcd: C, 39.65; H, 4.35; N, 16.01. Found: C, 39.57; H, 3.83; N, 15.97. NMR data: ^{1}H NMR (D_2O) δ 8.81 (s, 2, N=CH), 8.41 (t, 1), 8.13 (d, 2, J = 7.8 Hz), 3.77 (m, 2, C–NH), 2.48 (m, 2), 2.02 (m, 2), 1.64 (m, 2), 1.43 (m, 2); ^{13}C NMR (DMSO-d_6) δ 162.5 (2), 152.3 (2), 142.2 (1), 129.9 (2), 67.0 (2), 29.7 (2), 23.8 (2). Internal references δ 4.8 of HDO for ^{1}H NMR and δ 39.5 of DMSO for ^{13}C NMR were used.

Tb^{3+} and Eu^{3+} complexes of the enantiomer *SS*-pydach were prepared similarly by using 1(*S*),2(*S*)-diaminocyclohexane.

Spectroscopic Measurements. Absorption spectra were obtained using a Hitachi U-3200 spectrophotometer. CD spectra were recorded on a Jasco J-40 spectropolarimeter. NMR measurements were performed using a Jeol GX-270 FT spectrometer.

High-resolution luminescence and circularly polarized luminescence spectra were measured on an instrument constructed in this laboratory as described elsewhere[11] using UV lines of an argon ion laser (Spectra Physics Model 2025-05) for excitation. Excitation spectra were recorded with a Hitachi F-4010 spectrofluorometer. Luminescence quantum yields were obtained on the same instrument using a 1 N H_2SO_4 solution of quinine sulfate as a standard (Φ = 0.55). Luminescence life times were determined by using an excimer laser (XeCl, Lambda Physik Model EMG101 MSC) as an excitation source and a digital storage oscilloscope (Iwatsu Model DS-6612).

Molecular Orbital Calculations. Electronic states of the macrocyclic ligand were calculated by the PPP-CI method[7] using a 16-bit PC-9801 computer and a program constructed by Kihara and Tokita.[8] The values of two-center electron repulsion integrals (γ_{rs}) were calculated on the basis of Nishimoto–Mataga's equation.[9] The variable β and γ method was employed using parameters taken from ref 10. Further, the following values are used in the calculations: ionization potentials, I_p(C) = 11.16 eV, I_p(N) = 14.12 eV; one-center electronic repulsion integrals, γ(C) = 11.13 eV, γ(N) = 12.34 eV. In the CI calculations, 16 one-electron excited states were considered.

Results and Discussion

We first tried to prepare the tetramethyl derivative of the macrocycle (pydach) by a condensation reaction of 2,6-diacetylpyridine and diaminocyclohexane in the presence of lanthanide ions. However the complexes of the tetramethylmacrocycle could not be obtained. The electrostatic repulsion between the methyl groups and the hydrogen atoms on the cyclohexane ring may be the principal reason that the reaction did not proceed.

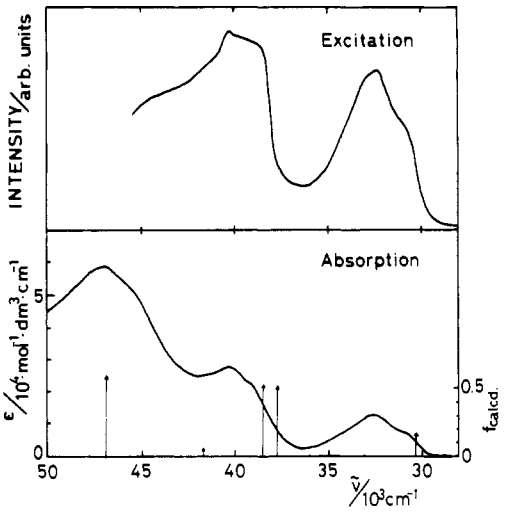

Figure 2. Absorption and excitation spectra of the Eu(*RR*-pydach)$^{3+}$ complex in methanol at room temperature. The calculated transition energy and oscillator strength of the chromophore are indicated by vertical arrows.

In the presence of lanthanide(III) nitrates, the template condensation of pyridine-2,6-dicarboxaldehyde and diaminocyclohexane yielded colorless crystals with moderate yields (33%–47%).

The complexes obtained have elemental compositions corresponding to Ln(*RR*-pydach)$(NO_3)_3 \cdot nH_2O$. The Shiff-base condensation was evidenced by the absence of the carbonyl stretching band and the presence of the imine band (1640 cm^{-1}) in the IR spectra.

NMR Spectra of La Complexes. NMR measurements were performed to obtain the structural information for the lanthanum complex. Although the macrocycle should have 26 carbon atoms, six sharp peaks and a sharp peak with half-intensity compared with the other peaks were detected in the ^{13}C NMR spectrum. The NMR result is reasonalbe if the structure of the macrocycle has D_2 symmetry at least on the NMR time scale, and the peak of half-intensity is ascribed to the carbon on the C_2 axis, i.e. the carbon atom located at the para position on the pyridine ring.

Absorption Spectra. The solution absorption and excitation spectra of Eu(*RR*-pydach)$^{3+}$ measured at room temperature are shown in Figure 2. The absorption spectrum shows three broad bands at 32.6 × 10^3, 40.3 × 10^3, and 47.0 × 10^3 cm^{-1} and shoulder peaks at 30.9 × 10^3 and 39.3 × 10^3 cm^{-1}. The locations and intensities of the bands are nearly identical with the absorption spectrum of Eu(pyMeen)$^{3+}$.[4] The absorption bands of Eu(*RR*-pybach)$^{3+}$ appearing in the near-UV region were reasonably ascribed to the π–π^* transitions within the ligand as demonstrated by MO calculations in this study. The UV absorption spectra of Tb(*RR*-pydach)$^{3+}$ and La(*RR*-pydach)$^{3+}$ can be superimposed on that of the corresponding Eu complex.

The excitation spectrum, corrected for photoresponse, was taken by monitoring the $^5D_0 \rightarrow {}^7F_2$ emission of Eu^{3+} at 16 800 cm^{-1}, and it is also presented in Figure 2. It is found that two strong bands with associated shoulders are located at the same wavenumbers as in the absorption spectrum. This indicates that an efficient energy transfer from ligand to the emitting level of Eu^{3+} occurs as it was reported for the Eu(pyMeen)$^{3+}$ complex. The excitation spectrum of Tb(*RR*-pydach)$^{3+}$, monitored at the $^5D_4 \rightarrow {}^7F_5$ emission line (18.4 × 10^3 cm^{-1}), also shows a 31 × 10^3 cm^{-1} band.

Molecular Orbital Considerations of the π-Electron System of the Ligand. In the macrocycle ligand pydach, there are two π-conjugated groups (N=C—C_5H_3N—C=N), which are reasonably regarded as chromophores in the pydach ligand. To investigate the nature of the π–π^* transitions, we calculated the energy of the π orbitals and the transition energy and moments by the PPP-CI method. Theoretical considerations were simplified on the electronic structure of macrocycles by calculating the electronic states of a chromophore (N=C—C_5H_3N—C=N). The

(7) (a) Pariser, R.; Parr, R. G. *J. Chem. Phys.* **1953**, *21*, 466. (b) Pariser, R.; Parr, R. G. *Ibid.* **1953**, *21*, 767.
(8) Kihara, H.; Tokita, S. *PPP-PC, Kinousei shikisono bunshi sekkei for NEC PC-9801 computer*; Maruzen: Tokyo, 1989.
(9) Nishimoto, K.; Mataga, N. *Z. Phys. Chem.* **1957**, *12*, 335.
(10) (a) Nishimoto, K.; Förster, L. S. *Theoret. Chim. Acta* **1966**, *4*, 155. (b) Nishimoto, K. *Ibid.* **1967**, *7*, 207.
(11) Morita, M.; Eguchi, K. *Sci. Pap. Inst. Phys. Chem. Res.* **1984**, *78*, 157.

Table I. Singlet Transition Energies, Oscillator Strengths (f), and Directions of Transition Moments of the π-Conjugated Chromophore N=C—C_5H_3N—C=N, Obtained by MO Calculation[a]

energy/10^3 cm^{-1}	f	direction of transition moment[b]
30.6	0.15	x
37.9	0.51	y
38.6	0.52	x

[a] Only the transitions of energies smaller than 50×10^3 cm^{-1} are listed. [b] The molecular structure and the definition of the coordinates are shown in Figure 5.

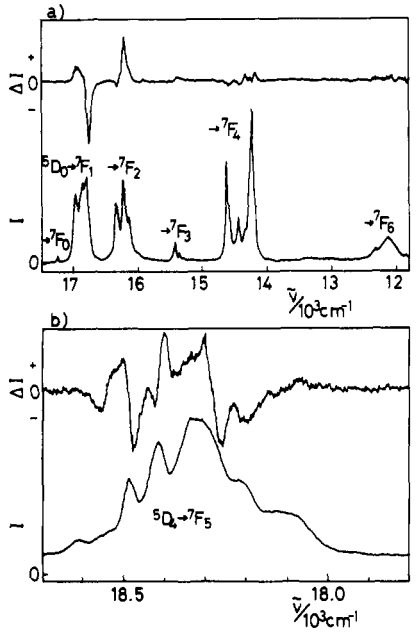

Figure 3. Luminescence and CPL spectra of (a) Eu(*RR*-pydach)$^{3+}$ and (b) Tb(*RR*-pydach)$^{3+}$ complexes in methanol at room temperature. The intensity of luminescence (I) and CPL (ΔI) are shown in arbitrary units.

results of the transition energy, strength, and the direction of the transition moments were tabulated in Table I. The calculated values of the energy and relative intensity of the transitions were also compared in Figure 2. The values of calculated energy coincide well with the observed ones if the vibrational broadening of the spectra is considered. The direction of the transition moment of the lowest energy singlet transition was along the long axis of the chromophore. The second and third transitions were revealed to have the transition moments along the short and long axis, respectively. Therefore the 32.6×10^3 cm^{-1} band of pydach should be ascribed to the long-axis-polarized transition.

Luminescence Spectra. The luminescence spectrum of the Eu(*RR*-pydach)$(NO_3)_3$ complex at room temperature is shown in Figure 3. The spectrum reveals the sharply split $^5D_0 \rightarrow ^7F_J$ transitions ($J = 0, 1, 2...$). It is noteworthy that the luminescence intensities of the $^5D_0 \rightarrow ^7F_1$ and $^5D_0 \rightarrow ^7F_4$ transitions are relatively high. A very weak but distinct peak was found in the $^5D_0 \rightarrow ^7F_0$ region, so that the presence of only one Eu complex in solution can be suggested. The strong luminescence peaks for the $\Delta J = 2$ and 4 transitions are good evidence for a lack of an inversion symmetry by selection rules.

The coordination site symmetry around the Eu^{3+} ion can be predicted by the number of splittings in the $^5D_0 \rightarrow ^7F_J$ transitions.[12] The observation of three components in the $^5D_0 \rightarrow ^7F_1$ transition clearly shows that the Eu^{3+} complex has a nonaxial symmetry, because the $^7F_1$ level of a Eu^{3+} complex of axial symmetry (including C_3 or higher symmetry axis) should consist of only one or two components. Since the macrocyclic ligand used in this study has chirality, we want to consider only chiral point groups. The presence of a C_2 axis should be assumed because NMR results confirmed the C_2 symmetry axis for the La^{3+} complex. Therefore we can assume either one of the two following point symmetry groups for the Eu^{3+} site symmetry: C_2 and D_2. The ^7F_J energy levels of the Eu^{3+} ions in C_2 and D_2 site symmetry are split into $2J + 1$ crystal field components. Between the $^5D_0$ and ^7F_J states, the same selection rules are applicable for both magnetic and electric dipole transitions irrespective of the considering symmetry groups, C_2 or D_2. Similarly, the following discussion can also apply to the CPL spectra concerning the number of the split peaks and the symmetry of the complex. In the C_2 crystal field, all of the electric dipole and magnetic dipole transitions between the $^5D_0$ and ^7F_J components are allowed; i.e., three peaks in $^5D_0 \rightarrow ^7F_1$, five peaks in $^5D_0 \rightarrow ^7F_2$, seven peaks in $^5D_0 \rightarrow ^7F_3$, and nine peaks in $^5D_0 \rightarrow ^7F_4$ can occur. In D_2 symmetry, the number of allowed peaks is reduced; three in $^5D_0 \rightarrow ^7F_1$, three in $^5D_0 \rightarrow ^7F_2$, six in $^5D_0 \rightarrow ^7F_3$, and seven in $^5D_0 \rightarrow ^7F_4$ can occur. In the luminescence and CPL spectra of Eu(*RR*-pydach)$^{3+}$, we have observed three peaks in the $^5D_0 \rightarrow ^7F_2$ region. Therefore, we could assume D_2 symmetry around the Eu^{3+} ion. Although a $^5D_0 \rightarrow ^7F_0$ peak, which should be electrically and magnetically forbidden, was detected, we consider that the Eu^{3+} complex has nearly D_2 molecular symmetry. Similar discussions for symmetries near to D_2 symmetry were also presented for a chiral crown-ether complex.[13]

CD Spectra and Conformation of Ligand. Figure 4 shows the CD spectra of Tb(*RR*- and *SS*-pydach)$^{3+}$. The spectra of two enantiomers are mirror images of each other. Eu(*RR*-pydach)$^{3+}$ and La(*RR*-pydach)$^{3+}$ gave nearly identical spectra with the corresponding Tb^{3+} complexes. All these spectra show positive and a negative Cotton effects in the spectral region at which the absorption band of comparatively strong intensity ($\epsilon \sim 10^4$) exists. This CD spectral pattern can be interpreted as a result of the exciton coupling of two chromophores which are chirally located with respect to each other.[14] This is illustrated as a twisted model in Figure 5b. In the pydach ligand, the excitonic interaction of two N=C—C_5H_3N—C=N chromophores (Figure 5a) can be considered. As shown in Figure 4, there is a negative band in lower energy side (30×10^3 cm^{-1}) and a positive band in the higher energy side (32.5×10^3 cm^{-1}) for the *RR*-pydach complex, due to "negative exciton coupling".[14] Therefore it is concluded from theory[14] that the transition moments of two chromophores are located at counterclockwise-twisted positions.

The direction of the transition moment of the absorption transition at 30×10^3 cm^{-1} is along the long axis of the chromophore as deciced by MO calculation. The interaction of the transition moments along the long axis generates chiral excitonic coupling. Therefore, the results of the CD spectra of *RR*-pydach complexes show that the ligand has a counterclockwise-twisted conformation,[14] as shown in Figure 5b. The conformation of the *SS*-pydach ligand should be opposite, that is, the clockwise-twisted form.

CPL Spectra and the Chirality of the Complexes. Information concerning the chirality of the complexes can also be drawn from the CPL spectra shown in Figure 3. We have confirmed that the enantiomer Eu(*SS*-pydach)$^{3+}$ complex shows a CPL spectrum which is an mirror image of the spectra of Eu(*RR*-pydach)$^{3+}$. Dissymmetry factors, $g_{em} = 2(I_L - I_R)/(I_L + I_R)$, and the position at the largest CPL peak in the each $^5D_0 \rightarrow ^7F_J$ band are as follows for the Eu(*RR*-pydach)$^{3+}$ complex: −0.19 (at 16.77×10^3 cm^{-1} in the $^5D_0 \rightarrow ^7F_1$ transition), 0.15 (16.23×10^3 cm^{-1} in $^5D_0 \rightarrow ^7F_2$), 0.17 (15.37×10^3 cm^{-1} in $^5D_0 \rightarrow ^7F_3$), −0.22 (14.62×10^3 cm^{-1} in $^5D_0 \rightarrow ^7F_4$). The largest dissymmetry factor 0.19 was observed at 16 780 cm^{-1} in the $^5D_0 \rightarrow ^7F_1$ transition. This transition is predicted to be the most prominent CPL transition from Richardson's theory[15] of selection rules. The large dissymmetry factors of the complex, in the range of $\sim 10^{-1}$ for all CPL peaks, indicate strong chiral environments around the central metal ion.

(12) Yatsimirskii, K. B.; Davidenko, N. K. *Coord. Chem. Rev.* **1979**, *27*, 223.
(13) Metcalf, D. H.; Carter, R. C.; Ghirardelli, R. G.; Palmer, R. A. *Inorg. Chem.* **1986**, *25*, 2175.
(14) Harada, N.; Nakanishi, K. *Circular Dichroic Spectroscopy-Exciton Coupling in Organic Stereochemistry*; University Science Books and Oxford University Press: Mill Valley, CA and Oxford, England, 1983.
(15) Richardson, F. S. *Inorg. Chem.* **1980**, *19*, 2806.

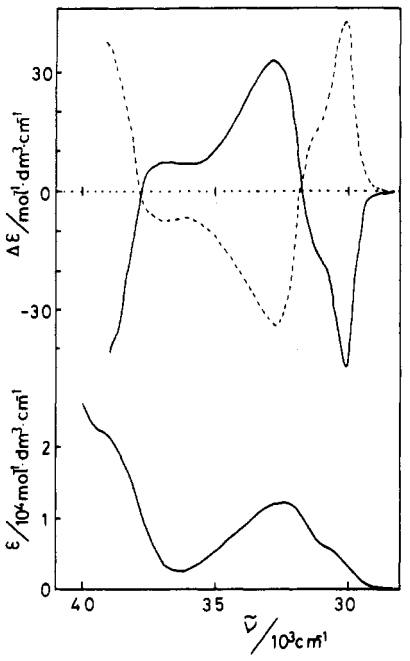

Figure 4. CD and absorption spectra of (—) Tb(*RR*-pydach)$^{3+}$ and (---) Tb(*SS*-pydach)$^{3+}$ complexes in methanol at room temperature.

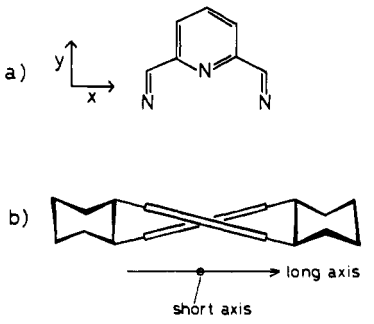

Figure 5. (a) Structure of the chromophore. (b) Twisted-structure model of the *RR*-pydach ligand. Two chromophores are shown to be oriented at counterclockwise positions.

The luminescence and CPL spectra of the Tb(*RR*-pydach)$^{3+}$ complex are partly shown in Figure 3b. The strong $^5D_4 \rightarrow {}^7F_J$ bands centered at 18.3×10^3 cm^{-1} are shown as usual in the luminescence spectrum. Sharply split and intense CPL peaks are observed in the $^5D_4 \rightarrow {}^7F_5$ band. The maximum g_{em} is −0.17 at 18 484 cm^{-1}. CPL peaks of exactly opposite signs and the same intensities were detected for the *SS*-pydach complex. The large dissymmetry factor also indicates a strong chiral environment at the Tb^{3+} ion as also seen for the Eu^{3+} complex.

Metcalf et al.[13] interpreted the luminescence and CPL spectra of the [Eu^{III}((all-*R*)-tetramethyl-18-crown-6)$(NO_3)_2$]$^+$ complex in terms of effective D_2 electronic symmetry. They reported that the biaxial and chiral crystal fields also involve the coordination of two nitrate anions. In the case of the *RR*-pydach complexes, however, the coordination of nitrate ions is unlikely because, in addition to the hexadentate macrocycle, the coordination of about three water molecules is also found, as it will be described in the following section. These results indicate that the strongly staggered conformation of the *RR*-pydach ligand itself generates biaxial and chiral environments for the central Eu^{3+} ion.

Lifetime, Quantum Yield, and Energy Transfer. The decay curves of the luminescence of Eu(*RR*-pydach)$^{3+}$ were single exponential in both H_2O and D_2O solution. The lifetimes of the $^5D_0$ state in H_2O and D_2O are 310 μs and 1.6 ms, respectively. The results show that the $^5D_0$ state of the Eu^{3+} complex is partly quenched by vibronic coupling with the high-frequency O–H vibrations.[16] By using an empirical equation proposed by Horrocks,[17] the number of the H_2O molecules bound to the Eu^{3+} complex in solution is calculated to be 3 at room temperature.

Sabbatini et al.[4] reported the intramolecular energy-transfer process in the emission of Eu(pyMeen)$^{3+}$. They showed that at room temperature excitation energy in the ligand mainly decays nonradiatively,[4] but about 1% of the excitation energy is transferred to the central Eu^{3+} ion by a Förster-type dipole–dipole interaction. In the process, the triplet state of the ligand was assumed to be involved in the energy transfer to the $^5L_6$ state of the Eu^{3+} ion. For the case of Eu(*RR*-pydach)$^{3+}$, the spectroscopic results obtained in this study can be interpreted by the same mechanism involving the energy-transfer process from the ligand to the Eu^{3+} ion. The emission quantum yield of Eu(*RR*-pydach)$^{3+}$ in D_2O at room temperature was 0.04 under the excitation ligand at 300 nm. The value is 1 order of magnitude larger than that reported for the Eu(pyMeen)$^{3+}$ complex. The emission lifetimes of the two Eu^{3+} complexes are nearly the same, which are 1.6 ms and 2.1 ms for Eu(*RR*-pydach)$^{3+}$ and Eu(pyMeen)$^{3+}$, respectively. Therefore, we would conclude that the relatively high emission quantum yield of Eu(*RR*-pydach)$^{3+}$ is not due to the high emission rate of the f–f transition in the Eu^{3+} ion but to the relatively high energy transfer rate from the macrocyclic ligand to the Eu^{3+} ion.

A similar energy-transfer mechanism can be proposed for the emission of the Tb^{3+} complex. A part of the energy of the excited state of the ligand must transfer to $^5D_3$ or some higher excited states of the Tb^{3+} ion and then be internally converted to the emissive $^5D_4$ state. However, some differences between the Tb^{3+} and Eu^{3+} complexes were observed. The decay curves of the Tb(*RR*-pydach)$^{3+}$ complex were non-single exponential in both H_2O and D_2O and included a fast decay ($\sim 10^{-6}$ s) component. The emission quantum yield in D_2O of the Tb(*RR*-pydach) complex was 2×10^{-2}, which is half that of the corresponding Eu^{3+} complex. The result can be interpreted as being due to a quenching process involving a back-energy-transfer from Tb^{3+} ion to the ligand. Sabbatini et al. also reported a broad emission (centered at 22.7×10^3 cm^{-1}) of a triplet state of the ligand, pyMeen, at low temperature.[4] The broad band spread from 18×10^3 cm^{-1} to 27×10^3 cm^{-1}. The results of the decay curves and the quantum yield of Tb(*RR*-pydach)$^{3+}$ could be explained by a back-energy-transfer from the emissive $^5D_4$ state of the Tb^{3+} ion to the triplet state of the ligand. On the other hand, the $^5D_0$ emissive state of the Eu^{3+} complex is far lower than the $^5D_4$ state of the Tb^{3+} complex, so that such back-energy-transfer cannot occur. If we assumed such a back-transfer process, the non-single exponential decay of Tb^{3+} is understandable.

Photochemistry. In the course of the luminescence experiments, a broad luminescence at around 23×10^3 cm^{-1} was found for Eu^{3+}, Tb^{3+}, and even La^{3+} *RR*-pydach complexes at room temperature. The intensity of the broad-band luminescence increased in proportion with the number of XeCl excimer laser shots at 308 nm. A similar broad band was observed in the luminescence spectrum of the aqueous solution of pyridine-2,6-dicarboxaldehyde alone after excimer laser radiation. Therefore, it is concluded that the C=N bonds in the macrocyclic ligand are dissociated by UV radiation and that the ligand is decomposed to pyridine-2,6-dicarboxaldehyde and diaminocyclohexane under excimer laser irradiations. We would consider the photoreaction products of pyridine-2,6-dicarboxaldehyde are the origin of this blue luminescence.

Conclusion. Spectroscopic results revealed that the pydach complexes have D_2 symmetry around the central Ln^{3+} ions. The macrocycle ligand has twisted chiral conformation (counterclockwise for the *RR*-pydach ligand). A part of the excitation energy is transferred from the surrounding ligand to the Eu^{3+} or Tb^{3+} ions, and then the emission from the excited f–f states of these ions can be observed. For the case of the Tb^{3+} complex, excited energy in the $^5D_4$ state is partially back-transferred to the ligand triplet state. Under intense UV laser radiation, these complexes were found to show interesting photodecomposition processes.

(16) Reference 1a, p 198.

(17) Horrocks, W. D., Jr.; Sudnick, D. R. *J. Am. Chem. Soc.* **1979**, *101*, 334.